ELSEVIER

Contents lists available at ScienceDirect

Soil Biology and Biochemistry

journal homepage: www.elsevier.com/locate/soilbio





Stimulation of soil gross nitrogen transformations and nitrous oxide emission under Free air CO₂ enrichment in a mature temperate oak forest at BIFoR-FACE

Fotis Sgouridis ^a, Michaela Reay ^{b,c}, Suparat Cotchim ^{b,d}, Jiaojiao Ma ^b, Aleksandar Radu ^e, Sami Ullah ^{b,*}

- ^a School of Geographical Sciences, University of Bristol, UK
- b Birmingham Institute of Forest Research and School of Geography, Earth and Environmental Science, University of Birmingham, UK
- ^c Organic Geochemistry Unit, School of Chemistry, University of Bristol, UK
- ^d Department of Chemistry, Prince of Songkla University, Thailand
- ^e Joseph Banks Laboratories, School of Chemistry, University of Lincoln, UK

ARTICLE INFO

Keywords: CO_2 fumigation FACE Nitrous oxide Mineralisation Denitrification Nitrification

Mature forest

ABSTRACT

Forest ecosystems are considered globally important sinks for offsetting increasing anthropogenic atmospheric carbon dioxide (CO2), however, this may be limited by the soil nutrient supply, predominantly nitrogen and phosphorus. Uncertainty remains regarding how soil N cycling in mature forests may respond to changes in carbon availability, arising from enhanced photosynthesis under elevated CO₂ (eCO₂) due to lack of experimental data. Further, potential positive feedbacks of nitrous oxide emissions may offset benefits of additional carbon sequestration under eCO2. The Birmingham Institute of Forest Research Free Air Carbon Enrichment experiment (BIFOR-FACE) started fumigating a mature temperate deciduous forest in 2017 at +150 ppm CO₂ above ambient. Soil N cycling responses to eCO₂ were investigated using the ¹⁵N pool dilution approaches to assess gross N mineralisation, immobilisation and nitrification rates, in combination with the ¹⁵N-gas flux method to quantify and source partition N2O production from 2018 to 2020 (2nd to 4th year of fumigation). Soil gross N mineralisation increased by 20% under eCO₂ (6.6 μ g N g⁻¹ d⁻¹) compared to the control treatment (5.3 μ g N g⁻¹ d⁻¹) and despite the trends being consistent over the three years (2018-2020), the high variability between arrays reduced statistical significance except in 2019. Ammonium immobilisation by microbes increased by 20% under eCO_2 (3.5 μg N g^{-1} d^{-1}) as well. Overall, gross mineralisation was 4 times higher than nitrification, indicating a much higher ammonium turnover rate compared to nitrate (1.5 vs. 12 days mean residence time). N₂O emission from denitrification $(0.18 \text{ ng N g}^{-1} \text{ h}^{-1})$ was significantly higher under eCO₂. After four years of CO₂ fumigation, there are modest indications of enhanced soil N transformation rates and N availability to support the observed enhanced canopy CO₂ uptake. Increased N₂O fluxes under eCO₂ indicated the potential for positive feedbacks on C sequestration under rising atmospheric CO2. The overall implications for C sequestration will depend on how long upregulation of soil N transformations and N bioavailability will last to meet plant demands before manifestation of N limitation, if any.

1. Introduction

Forest ecosystems are key to the global carbon (C) sink, representing $\sim 30\%$ of the total global area (Keenan et al., 2015). Within this, temperate forests contribute 0.72 ± 0.08 Pg C year⁻¹ to the forest C sink containing 0.66 trillion trees (Crowther et al., 2015; Pan et al., 2011). With increasing atmospheric CO₂ concentrations worldwide (currently

surpassing 415 ppm), the importance of this sink to offset increasing anthropogenic CO₂ is of global interest (Friedlingstein et al., 2020). A recent data-driven review of plant biomass response to eCO₂ indicated the ability of forests to act as a C sink was controlled by plant available nitrogen (N) and phosphorus (P) (Terrer et al., 2019). Thus, it is essential to determine how nutrient cycling is affected by increasing atmospheric CO₂. Free Air Carbon Enrichment (FACE) experiments can provide the

E-mail address: s.ullah@bham.ac.uk (S. Ullah).

^{*} Corresponding author.

necessary realistic experimental manipulation environments to assess response of ecosystems to enriched atmospheric CO₂ concentrations (Hendrey et al., 1999). These operate on a system-level, enabling insights into whole ecosystem response, yielding both empirical and mechanistic information at a vegetation and soil level (Ainsworth and Long, 2005; Norby et al., 2016).

Forest FACE experiments have shown consistent photosynthetic enhancements (Ainsworth and Rogers, 2007; Nowak et al., 2004) and subsequent increases in C allocation belowground. This includes increase in fine root production in young forests, linked to greater exploration of soil to access additional nutrients (De Graaff et al., 2006; Dieleman et al., 2010; Jackson et al., 2009; Phillips et al., 2012). In a mature forest setting, no change was observed in root carbon allocation during initial years of fumigation in a P-limited eucalyptus forest, where greater exploration of forest soil has already occurred compared with plantation forests (Jiang et al., 2020; Piñeiro et al., 2017). Increased root exudation under eCO2 may also supply low-molecular-weight C belowground (Delucia et al., 1997; Fransson and Johansson, 2010; Johansson et al., 2009; Phillips et al., 2009). An increase in belowground C availability can concurrently increase nutrient mobilisation, via priming effects on the microbial community, promoting microbial turnover, and litter and soil organic matter (SOM) decomposition (Dijkstra et al., 2013; Hoosbeek et al., 2004; Jilling et al., 2021; Kuzyakov, 2002). There has been extensive investigation of N cycling processes under eCO₂, including meta-analyses (De Graaff et al., 2006; Rütting and Andresen, 2015; Zak et al., 2003). The response of N cycling processes, including mineralisation, ammonium (NH₄⁺) consumption, and nitrification have been variable. However, an overall increase in young forest FACE experiments, using response ratios, has indicated mineralisation and immobilisation are stimulated to a similar degree under eCO2 (Rütting and Andresen, 2015). Additionally, increases in mineralisation under eCO2 have been linked to N limitation, with Rütting and Andresen (2015) proposing in N limited settings, enhanced root exudation will stimulate N mineralisation. Conversely, in P limited settings, despite increases in nutrient availability in the rhizosphere, limited effects on N transformations under eCO2 have been observed, which is supported by the only study in mature Eucalyptus dominated forest, which is mainly a P-limited forest (Euc-FACE) (Andresen et al., 2020; Ochoa-Hueso et al., 2017; Rütting and Andresen, 2015). Upregulation of nitrogen cycling processes, particularly in N-limited northern temperate forests, is essential to sustain increased plant growth. Furthermore, there have been observations of progressive nitrogen limitation, with subsequent down-regulation of plant growth, however, these are limited to young forests (Luo et al., 2004; Norby and Zak, 2011). Whilst northern temperate forests in the western hemisphere have been exposed to enhanced atmospheric reactive nitrogen (Nr) deposition in the 20th century, the contemporary gradual decline in Nr deposition since 2000 coupled with increasing atmospheric CO2 is likely to result in progressive nitrogen limitation. Thus, evaluating the responses of N cycling to eCO2 is critical to discern whether CO2 uptake might be limited by N availability.

When considering changes in N transformations in ecosystems under eCO₂ to support C sequestration, there is potential for positive feedback on greenhouse gas emissions as nitrous oxide (N₂O), given that substrate supply for nitrification and denitrification is regulated by N immobilisation and mineralisation, and labile C availability (Kammann et al., 2008; Knowles, 1982). Any increases have the potential to partially offset benefits of additional C stored, as N₂O has a global warming potential of 298 times higher than that of CO_2 (van Groenigen et al., 2011). Previous meta-analysis of all ecosystems under eCO₂ showed an increase of 18.8% (van Groenigen et al., 2011), however, studies related to forests, particularly mature forests are limited. In young forests, studies have found no significant changes in N₂O flux under eCO₂, despite seasonal difference between ambient and elevated CO_2 , driven by plant N uptake (Ambus and Robertson, 1999; Hagedorn et al., 2000; Phillips et al., 2001). In settings where conditions were optimal for N₂O

production under eCO₂, including increased NO_3^- production, in open top chambers planted with *Pinus sylvestris* seedlings, potential denitrification, net nitrification and N_2O flux increased (Carnol et al., 2002). However, there is yet to be a study for mature temperate forest to quantify potential N_2O production and its major microbial sources. In largely aerobic forest soils, the main sources of N_2O are expected to be the heterotrophic denitrification of nitrate but also the oxidation of ammonium derived from the mineralisation of organic nitrogen (Sgouridis and Ullah, 2017).

The Birmingham Institute of Forest Research FACE experiment (BIFoR-FACE) has been fumigating a mature oak dominated forest in Staffordshire since spring 2017 at +150 ppm above the ambient (Hart et al., 2020; MacKenzie et al., 2021). This is a mature temperate forest dominated by oak (Quercus robur) in the upper canopy, and being typical of temperate forests, is considered N limited, although the contemporary atmospheric Nr deposition might have alleviated the N limitation. The Nr disposition has been in decline in the UK in the last three decades (Tipping et al., 2017) and thus it is likely that these forests will revert to a more tight N cycling, particularly under increasing atmospheric CO2 in future. In the first three years of CO2 fumigation, the oak canopy exhibited a maximum of 33 \pm 8% increase in light-saturated net photosynthetic rates (Asat), with no decline in leaf nitrogen, despite an increase in leaf mass per unit area (Gardner et al., 2021, 2022). These results indicated that provided there are adequate nutrients, there will be a sustained enhancement of C assimilation (Gardner et al., 2022). Thus, the question of how N availability is sustained to maintain the enhanced C sink at BIFoR-FACE arises. To investigate N availability and transformations, we used ¹⁵N pool dilution to assess gross N mineralisation, immobilisation and nitrification rates, in combination with the ¹⁵N-gas flux method to quantify and source partition N₂O (Sgouridis et al., 2016) from 2018 to 2020 at BIFoR-FACE. We hypothesised that (I) gross N mineralisation and immobilisation will increase to meet plant and microbial N metabolic demands and (ii) that N2O flux will decrease, due to increased competition for available N by plants and microbes.

2. Methods

2.1. Study site and sampling strategy

The Birmingham Institute of Forest Research (BIFoR) established a Free-Air CO_2 Enrichment (FACE) facility in 2017 in a mature temperate oak dominated forest to study under 'real world' conditions the effects of CO_2 fertilisation on forest ecosystems and the services they provide. The woodland is located in Staffordshire (UK) and is dominated by *Quercus robur* (pedunculate oak) in the upper canopy, with a *Corylus avellana* (common hazel) coppice understorey. There is variable coverage of brambles (*Rubus* sp.) and ferns where the canopy is not closed. The FACE experiment was set up in 2017 in 6 circular arrays following a paired experimental design (Fig. 1); arrays 1, 4 & 6 are receiving 150 ppm of CO_2 above ambient (e CO_2 arrays) at canopy level during the growth season alone and were paired based on similar dominant tree species composition and broader soil texture (for details see Hart et al. (2020)) with arrays 3, 2 and 5 (a CO_2 control arrays) which are not receiving CO_2 fumigation.

Soil samples were collected on 3 occasions in May 2018, in May 2019 and in August 2020 (delayed sampling due to the pandemic lockdowns), to represent the soil conditions and nitrogen cycling activity at the late spring-summer growth stage. Soils were collected using a 20 cm deep hand auger after removing any surface litter and inserting the auger at $\sim\!15$ cm depth, therefore aggregating the O (usually $\sim\!6-8$ cm deep) with the A horizon. There are 3 soil sampling subplots in each array that were sampled at 2-2-1 frequency to yield 5 replicate soil samples per array (n=30 per sampling campaign). It should be noted that the replicated soil samples should be considered as technical or field replicates, but not $\rm CO_2$ treatment replicates. The samples were transported to the laboratory on ice and stored at 4 °C between one and two weeks before further

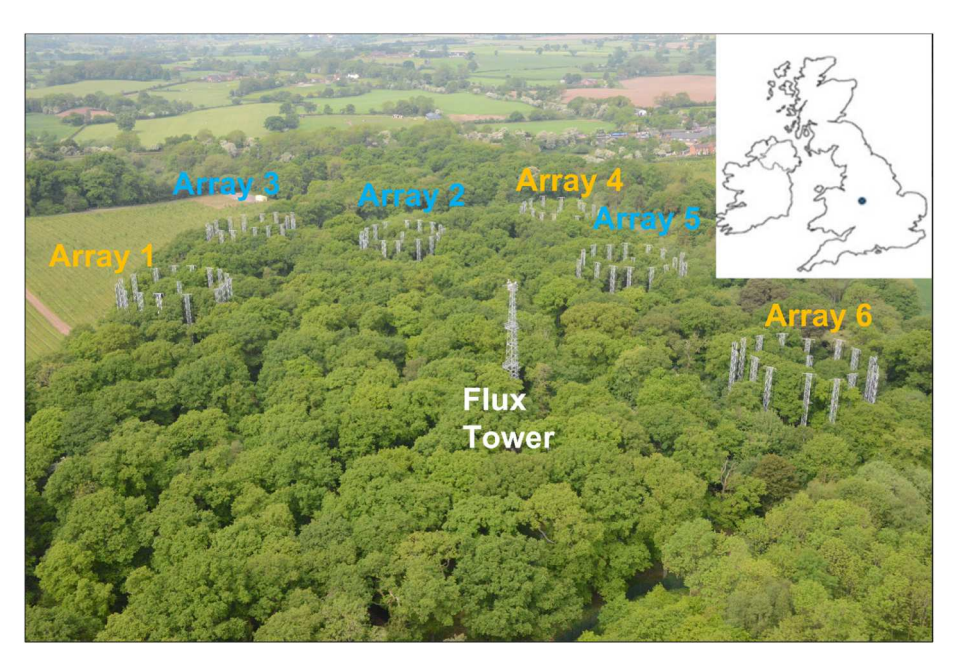


Fig. 1. Aerial view of the FACE arrays experiment in Staffordshire UK. Fumigated (eCO₂) arrays are highlighted in orange and control (aCO₂) arrays are highlighted in blue

processing.

2.2. Soil geochemical properties

Prior to any geochemical analysis each soil sample was manually homogenised, and sieved (<2 mm) at field moisture, therefore removing any large roots and stones. Soil moisture was then determined gravimetrically by drying at 105 °C for 24 h and until constant weight. Homogenised field moist soils (1 g) were extracted at a ratio of 5:1 with 5 mL 2 M KCl for the determination of exchangeable ammonium (NH₄) and nitrate (NO₃), while 5 g were extracted with 25 mL of deionised water for the determination of dissolved organic carbon (DOC) and total dissolved nitrogen (TN), and major anions and cations. The soil slurries were continuously shaken on a reciprocating shaker at 200 rpm for 1 h before being centrifuged at 5000 rpm for 10 min followed by filtration with 0.22 µm 25 mm PES syringe filters. Ammonium was analysed spectrophotometrically on a Gallery Plus Automated Photometric Analyser (Thermo Fisher Scientific, UK) using a salicylate-hypochlorite alkaline reaction method measured at 660 nm, and nitrate using a vanadium reaction method measured at 540 nm. The limits of detection were $0.005 \text{ mg L}^{-1} \text{ NH}_4^+\text{-N}$ and $0.010 \text{ mg L}^{-1} \text{ NO}_3^-\text{-N}$, the samples were blank corrected, while the precision as a relative standard deviation (RSD) was <2%.

Major anions and cations were measured simultaneously in the deionised water soil extracts using an ICS-5000 ion chromatograph (Thermo Fisher Scientific, UK). Anions were separated isocratically on an AS11-HC 2 mm column at 0.25 ml min⁻¹ flow rate using 24 mM KOH eluent. Cations were separated isocratically on an CS12 2 mm column at 0.25 ml min⁻¹ flow rate using 20 mM MSA eluent. The limit of detection was 0.001 mg L^{-1} for all measured anions and cations, the samples were blank corrected, while the precision as a RSD was <2%. DOC and TN concentrations were quantified simultaneously using a Shimadzu TOC-L Organic Carbon Analyser, with a total nitrogen module (TNM). Nonpurgeable organic carbon (NPOC) was measured after acidification of samples with 9 M H_2SO_4 and catalytic combustion (720 $^{\circ}\text{C})$ of dissolved organic carbon to carbon dioxide, which was then measured by infrared absorption (NDIR detector), whilst the produced NOx from the catalytic decomposition of TN was detected by a chemiluminescence detector. The limit of detection was 0.01 mg C $\rm L^{-1}$ and 0.005 mg N $\rm L^{-1}$, respectively, the samples were blank corrected, while the precision as a RSD was <5%.

The dried soils following the gravimetric soil moisture determination were pulverised with a pestle and mortar (<1 mm) and $\sim\!10$ mg subsamples were weighed in triplicate in tin capsules. These samples were subsequently analysed for elemental C & N contents as well as $\delta^{15}{\rm N}$ and $\delta^{13}{\rm C}$ stable isotopes via a continuous flow isotope ratio mass spectrometer (Elementar Isoprime Precision; Elementar Analysensysteme GmbH, Hanau, Germany) coupled with an elemental analyser (EA) inlet (vario PYRO cube; Elementar Analysensysteme GmbH, Hanau, Germany). The EA was calibrated with sulfanilamide (N: 16.26%, C:41.81%, S: 18.62%) and the precision as a RSD was <5% for both C and N. The IRMS was calibrated against international reference standards (caffeine: USGS61 (-2.87% $\delta^{15}{\rm N}$, -35.05% $\delta^{13}{\rm C}$ VPDB), USGS62 (20.17% $\delta^{15}{\rm N}$, -14.79% $\delta^{13}{\rm C}$ VPDB), USGS63 (37.83% $\delta^{15}{\rm N}$ -1.17% $\delta^{13}{\rm C}$ VPDB) and the precision as a standard deviation (SD) was <0.06% for both $\delta^{15}{\rm N}$ and $\delta^{13}{\rm C}$ stable isotopes.

2.3. Experimental design

2.3.1. Gross nitrogen transformations

Within 1-2 weeks from each sample collection, field moist, homogenised soils were used in a laboratory incubation with 15N-NH₄ and ¹⁵N-NO₃ to determine gross mineralisation and nitrification rates, respectively according to the isotope pool dilution technique (Davidson et al., 1992; Hart et al., 1994). Approximately 10 g of each field moist soil sample was weighed in quadruplicate acid washed and furnaced 120 mL volume serum bottles. Two of each replicates received 0.5 ml labelled $\rm K^{15}NO_3^-$ (98 at. % $\rm ^{15}N$, Sigma-Aldrich) and the other two received 0.5 ml labelled $\rm ^{15}(NH_4)_2SO_4$ (98 at. % $\rm ^{15}N$, Sigma-Aldrich). The tracer solution (volume adjusted within 5% of the ambient soil volumetric water content) was applied in the serum bottles via multiple injections of equal volume using a hypodermic syringe and needle. The concentration of the tracer for each soil sample was prepared with the aim to enrich the soil N pool (either NO₃ or NH₄) up to 20 at%. Immediately after the addition of the ¹⁵N tracer one replicate of the two for each treatment (t₀ samples) was extracted with 50 ml 2 M KCl and 5 ml aliquots of the soil extracts were frozen at $-20~^{\circ}$ C until colorimetric analysis for NO₃ and NH₄ as described above. The other two labelled replicates were stoppered with butyl rubber septa and were incubated in the dark at 20 °C for 24 h. After the end of the incubation and before

opening the serum bottles, headspace gas samples (20 ml) were collected with a gas-tight syringe and transferred in 12 ml pre-evacuated borosilicate gas-tight exetainer vials (Labco, Ceredigion, UK). Following gas sampling, the serum bottles (t $_{24}$ samples) were opened and then extracted in the same way as the t_0 samples. Approximately 40 ml of the 2 M KCl soil extracts were used for the two-step $^{15}\text{N-NH}_4^+$ and $^{15}\text{N-NO}_3^-$ diffusion procedure as described by Brooks et al. (1989), with the modification of enclosing the filter disks in a 0.2 μm Teflon membrane, which was then left to float on the surface of the soil extract within each gas-tight diffusion cup during the 6-day diffusion period. The diffusion filter disks were analysed for ^{15}N content using the EA-IRMS set up described earlier.

Gross mineralisation and nitrification rates were estimated from changes in atom percentage of ^{15}N excesses (APE) above natural background and N-pool size differences between t_0 and t_{24} samples using the equations developed by Kirkham and Bartholomew (1954). The NH $_{1}^{+}$ immobilisation rate was estimated by subtracting the gross nitrification rate from the gross NH $_{1}^{+}$ consumption rate, while the gross NO $_{3}^{-}$ consumption rate, when the incubation conditions do not favour denitrification (Hart et al., 1994).

2.3.2. Partitioning of nitrous oxide emissions

The headspace gas samples collected during the lab incubations for gross nitrogen transformations were used to quantify N2O emission and apportion its sources to denitrification (when K¹⁵NO₃ tracer was used) and nitrification (when ¹⁵(NH₄)₂SO₄ tracer was used) (Ambus et al., 2006; Matson et al., 2009). The ¹⁵N content of the N₂O in the 12 mL exetainer vials was determined using a continuous flow isotope ratio mass spectrometer (Elementar Isoprime Precision; Elementar Analysensysteme GmbH, Hanau, Germany) coupled with a trace-gas pre-concentrator inlet with autosampler (isoFLOW GHG; Elementar Analysensysteme GmbH, Hanau, Germany). Gas samples in 12 ml exetainers were purged into a He stream through the autosampler and after passing through a CO₂ and a H₂O scrubber, then entered a first liquid N₂ trap isolating and cryofocusing the N2O. Following the initial N2O trapping, N_2 was subsampled through a 7 μl sub-sampling loop and after O₂ reduction through a Cu reduction furnace at 600 °C, the N₂ was directed to the IRMS where the N_2 isotopologues ($^{28}N_2$, $^{29}N_2$, and $^{30}N_2$ respectively) as well as the ratios R29 ($^{29}N_2/^{28}N_2$) and R30 ($^{30}N_2/^{28}N_2$) were measured at a trap current of 100 μ A in both enriched (t_{24} samples) and reference samples (to samples). The rest of the gas sample was further concentrated in a second liquid N₂ trap and the isolated N₂O was further separated from any residual CO2 by passing through a Poraplot Q gas chromatography column before being directed to the IRMS where the N_2O isotopologues ($^{44}N_2O$, $^{45}N_2O$, and $^{46}N_2O$ respectively) as well as the ratios R45 ($^{45}N_2O$ / $^{44}N_2O$) and R46 ($^{46}N_2O$ / $^{44}N_2O$) were measured at a trap current of 600 μ A in both enriched (t_{24} samples) and reference samples (t₀ samples). Instrument stability checks were performed prior to each analysis by running a series of 10 reference pulses of pure N2 and N_2O (BOC special gases) until a standard deviation of $\delta^{15}N$ better than 0.05‰ was achieved.

Additionally, six consecutive atmospheric air samples in 12 ml exetainers were analysed prior to the analysis of actual samples. The minimum detectable change (MDC) in R29 and R30 was defined from the air reference standards (n=6) and was calculated using the following equation (Sgouridis et al., 2016):

$$MDC = \mu_{pair\ diff} + (2\sigma_{pair\ diff}) \tag{1}$$

where μ is the mean difference of all possible unique pairs of air reference standards (n=15) and σ is the standard deviation between sample pairs. The MDC for R29 was 3.9×10^{-6} and for R30 was 8.2×10^{-7} and these values were used to determine if each time step sample was significantly different from ambient reference samples (t_0 samples) and if not they were excluded from the flux calculations. Due to the low

enrichment (20 15 N at%) targeted for the gross nitrogen transformations, the t_{24} samples did not show any significantly enriched 15 N₂, above natural abundance, and therefore N₂ fluxes were not calculated and reported here.

The 'non-equilibrium' equations (Arah, 1997; Mulvaney, 1984) were applied for calculating the N2O fluxes, after correcting for the naturally occurring oxygen isotopes, as described in detail in Sgouridis and Ullah (2015). Therefore, after the oxygen correction the ratios R45 and R46 were converted to ratios of R29 and R30, and the MDC was defined according to equation (1), for the converted R29 and R30, as 6.8×10^{-5} and 3.1×10^{-5} , respectively. For calculating the $^{15}\text{N-N}_2\text{O}$ flux apart from the converted R29 and R30 ratios, measurement of the N_2O concentration in the t24 samples is also required. Therefore, the 12 ml exetainer vials, before being committed to IRMS analysis, which sweeps through the whole sample, were loaded on a PAL3 autosampler mounted on top of an Agilent 7890A gas chromatograph (Agilent Technologies Ltd, USA) equipped with µECD and FID detectors and 1 ml of gas was sub-sampled and analysed for N2O and the flux rate was determined by linear regression between 0 and 24 h. The instrument precision was determined from repeated analyses of 8 lab air samples and the RSD was <1%, while the limit of detection (LOD) was at 9 ppb N₂O.

2.3.3. Potential net N2O emission

In August 2020, a separate laboratory incubation was conducted to elucidate the effect of CO2 fumigation on soil greenhouse gas emissions without the addition of ¹⁵N-labelled tracers. Soils were sampled from all the arrays (0-20 cm) in August 2020 as above but limiting the soil replicate samples to 3 per array (n = 18). After homogenisation, 100 g of field-moist soil was weighed into duplicate 1000 ml acid washed Mason jars. Each replicate Mason jar received a soil moisture treatment, which was either adjusting all the soils to the average ambient moisture of 23% v/v at the time of soil sampling, or at 50% v/v high water content, using deionised water. The 23% treatment represented typical summer soil moisture on the site whilst the 50% treatment represented non-growing season (winter) moisture. This was done to elucidate impacts on potential GHG production during low (23%) and high (50%) moisture conditions. The jar lids were then capped, stoppered with butyl rubber septa and were incubated in the dark at 20 °C for 16 days. Gas samples (5 ml) were collected via syringe and needle through the septa at times 0, 2, 6 and 24 h on day 1, and at 0 and 2 h on days 2, 6, 9 and 16 into preevacuated 3.5 ml borosilicate exetainer vials (Labco, Ceredigion, UK). After each sampling, the sampled headspace gas was replaced with atmospheric air in order to maintain atmospheric pressure throughout the incubation period. The gas samples were analysed manually on an Agilent 7890A gas chromatograph (Agilent Technologies Ltd, USA) equipped with µECD for N2O detection. N2O fluxes were estimated by linear regression between the sampled time intervals as above.

2.4. Statistical analysis

Prior to any statistical tests the data were analysed for normality and homogeneity of variance with the Kolmogorov-Smirnov test and the Levene statistic respectively, but the assumptions for parametric tests were not met. Therefore, means comparisons of the soil variables and N transformation processes, for both annual and full datasets, was done using the non-parametric Mann-Whitney test. Principal Component Analysis (PCA) was used to explore the combinations of soil physicochemical properties, 'principal components', which are likely to provide the maximum discrimination between treatment arrays and the extracted principal components were used as independent variables in linear regression to explain the variance in key soil N transformation processes. Treatment differences in the greenhouse gas flux dataset were explored using two-sample t-test and Two-Way ANOVA for discriminating between the effect of fumigation, soil moisture and their combination. Non-parametric Spearman correlation was used instead of Pearson correlation between not normally distributed variables. All

statistical analyses were performed using SPSS® 24.0 for Windows.

3. Results

3.1. Soil properties

The fumigated soils displayed higher elemental carbon content (Table 1). This likely pre-existed the fumigation treatment, reflecting differences in the organic horizon depth across the forest. However, there was a marked increase in the more labile fraction, represented by the DOC and also acetate. The $\delta^{13}C$ signal was more depleted in eCO2 arrays, most likely as a result of the additional CO2 supply through fumigation, with an average $\delta^{13}C$ of $\sim\!18\%$ (measured at ground level) compared to atmospheric CO2 with $\delta^{13}C\sim-8\%$ (unpublished data). From the measured nitrogen species (oxidised and reduced), NH $_{+}^{+}$ content, N% and C/N ratio were statistically significantly higher under the eCO2 arrays providing a first indication that N cycling is very likely stimulated under CO2 fumigation. The average $\delta^{15}N$ of the eCO2 soils was marginally enriched, though statistically not different between the treatment and control arrays.

Interestingly, and despite the fact that all eCO $_2$ (fumigated) and aCO $_2$ (control) arrays were sampled on the same days, soil moisture was higher under eCO $_2$ even though the array selection and set up was aimed at similar soil conditions between the fumigation and control arrays. All the measured major ions were also higher in the fumigated soils, but the differences were significant only for Na $^+$, Cl $^-$ and acetate. It should be noted that inter-annual differences in soil properties were also observed and these may have been influenced by climatic differences and extreme events between the studied years (Supplementary Information; Table S1). However, the prevailing trends between fumigated and control arrays were consistent throughout the study period.

3.2. Gross nitrogen transformations

Mean gross mineralisation (p = 0.086) and gross nitrification rates (p = 0.102) were on average higher in eCO₂ compared to aCO₂ soils together with positive response ratios (Table 2); however, the differences were not statistically significant at 95% confidence, due to the

Table 1 Soil properties in eCO $_2$ (fumigated) and aCO $_2$ (control) arrays in the upper 15 cm soils (O horizon and part of A horizon) of the FACE oak woodland in Staffordshire. Data are means \pm SE of the three sampled growth seasons between 2018 and 2020. pH data are shown only for 2018, whereas for major ions data exist only from 2019 to 2020. *P* values < 0.05 indicate significant difference of the means between eCO $_2$ and aCO $_2$ treatments according to the Mann-Whitney test.

Soil properties	eCO_2	aCO_2	<i>p</i> -value
Gravimetric soil moisture (%) (n = 90)	37.1 ± 1.76	30.4 ± 1.74	<0.001*
NH_4^+ (µg N g ⁻¹ dry soil) (n = 90)	9.0 ± 1.11	6.7 ± 1.07	0.030*
NO_3^- (µg N g ⁻¹ dry soil) (n = 90)	21.1 ± 2.90	19.1 ± 2.65	0.250
N (%) $(n = 90)$	0.5 ± 0.05	0.4 ± 0.03	0.002*
C (%) $(n = 90)$	9.6 ± 0.95	6.0 ± 0.58	0.002*
C/N (n = 90)	17.1 ± 0.28	16.0 ± 0.24	0.004*
δ^{15} N (‰) ($n = 90$)	-0.6 ± 0.19	-0.9 ± 0.31	0.323
δ^{13} C (‰) ($n = 90$)	-28.8 ± 0.09	-28.3 ± 0.08	< 0.001*
DOC (μ g C g ⁻¹ dry soil) ($n = 90$)	331.2 \pm	256.0 \pm	0.006*
	26.18	22.26	
TN (μ g N g ⁻¹ dry soil) ($n = 60$)	63.0 ± 6.97	58.9 ± 6.68	0.329
pH ($n = 30$)	3.9 ± 0.02	3.8 ± 0.07	0.819
Na^{+} (µg g ⁻¹ dry soil) (n = 57)	50.8 ± 3.38	40.2 ± 4.19	0.002*
K^+ (µg g ⁻¹ dry soil)	47.6 ± 7.55	34.1 ± 5.84	0.106
(n = 57)			
Mg^{+} (µg g^{-1} dry soil) ($n = 57$)	$\textbf{7.2} \pm \textbf{0.98}$	6.7 ± 0.92	0.330
Ca^{2+} (µg g ⁻¹ dry soil) (n = 57)	28.3 ± 4.12	24.8 ± 4.26	0.141
Cl^{-} (µg g ⁻¹ dry soil) ($n = 57$)	24.1 ± 6.13	10.3 ± 0.77	0.001*
SO_4^{2-} (µg g ⁻¹ dry soil) (n = 57)	14.3 ± 0.99	13.3 ± 0.93	0.598
PO_4^{3-} (µg g ⁻¹ dry soil) ($n = 57$)	4.0 ± 1.43	4.3 ± 2.58	0.471
Acetate ($\mu g g^{-1}$ dry soil) ($n = 57$)	3.6 ± 0.47	1.9 ± 0.23	0.002*

Table 2 Soil nitrogen transformation rates in eCO $_2$ (fumigated) and aCO $_2$ (control) FACE arrays. Data are means \pm SE of the three sampled growth seasons between 2018 and 2020. *P* values < 0.05 indicate significant difference of the means between eCO $_2$ and aCO $_2$ treatments according to the Mann-Whitney test.

Nitrogen Transformations	eCO ₂	aCO ₂	<i>p</i> - value	Relative response
Gross Mineralisation ($\mu g \ N \ g^{-1}$	6.6 ±	5.3 ±	0.086	0.20
day^{-1}) ($n = 89$)	0.77	0.84		
Gross Nitrification (μg N g ⁻¹	$1.8~\pm$	1.4 \pm	0.102	0.22
day^{-1}) $(n = 88)$	0.43	0.45		
Ammonia consumption (µg N	$6.6 \pm$	5.4 \pm	0.195	0.19
$g^{-1} day^{-1}$) (n = 89)	0.81	0.82		
Ammonia Immobilisation (µg N	4.4 \pm	3.6 \pm	0.337	0.20
$g^{-1} day^{-1}$) ($n = 87$)	0.80	0.80		
Denitrification N ₂ O (ng N g ⁻¹	0.18 \pm	$0.10 \pm$	0.016*	0.54
h^{-1}) ($n = 90$)	0.051	0.033		
Nitrification N ₂ O (ng N g ⁻¹ h ⁻¹)	$0.08 \pm$	$0.04 \pm$	0.108	0.91
(n = 88)	0.033	0.014		

relatively high variability between the 3 sampling years (Fig. 2A&B). There was a significant inter-year variation in gross N transformations (see SI Appendix A for results of linear mixed effects models). Only in 2019, gross nitrification and ammonia consumption were significantly higher in fumigated soils (p < 0.05). Overall, gross mineralisation was 4 times higher than nitrification rates, indicating a much higher turnover rate of the ammonium pool in the soil. This finding is further corroborated when comparing the mean residence time (MRT) for the ammonium and nitrate pools, defined as ammonium pool divided by the gross mineralisation rate and nitrate pool divided by the gross nitrification rate, respectively. The MRT for the ammonium pool was on average 1.5 days, compared to the MRT for nitrate, which was 12 days, with the lower MRT indicating a more active pool, with faster turnover.

The gross ammonia consumption rate (Table 2 & Fig. 2C) was of similar magnitude and following the same trend as the gross mineralisation rate, while it was dominated by microbial ammonia immobilisation rather than nitrification. The ammonia immobilisation rate (Fig. 2D) represented 82% of the ammonia consumption (in the absence of plant uptake during our incubation conditions) in 2018, while this proportion reduced to 70% in 2019 and to 50% in 2020, which is probably due to the concurrent increase in gross nitrification rates from 2018 to 2020 (Fig. 2B & Table S2). Since no differences were observed between eCO2 compared to aCO2 arrays, the above relationships represent whole forest soil dynamics and differences between the investigated years. Finally, the nitrate consumption rate was on average negative, indicating insignificant nitrate immobilisation in these forest soils. Immobilisation of ammonium seems to have been favoured by microbes compared to nitrate. However, as shown in the next section, some of the available nitrate was also denitrified that may have limited immobilisation.

3.3. Nitrous oxide emission and source partitioning

Nitrous oxide emissions were consistently higher from eCO₂ soils both when nitrate was used as $a^{15}N$ tracer (denitrification as source) and also when ammonium (nitrification as source) was used as tracer. However, only denitrification derived N₂O was statistically higher in eCO₂ soils compared to aCO₂ across the whole dataset (Table 2), while statistical significance varied on annual basis as shown in Fig. 3 & Table S2. Potential N₂O emission from these soils was generally low, about 3–4 orders of magnitude lower than gross mineralisation and nitrification. Denitrification contributed twice as much N₂O compared to nitrification (Fig. 3), further corroborating the slower gross nitrification rates measured with the isotope dilution technique. It should be noted though, that direct comparison of process rates between denitrification and gross nitrification and mineralisation is not possible, since N₂ fluxes (the final and more quantitatively important product of

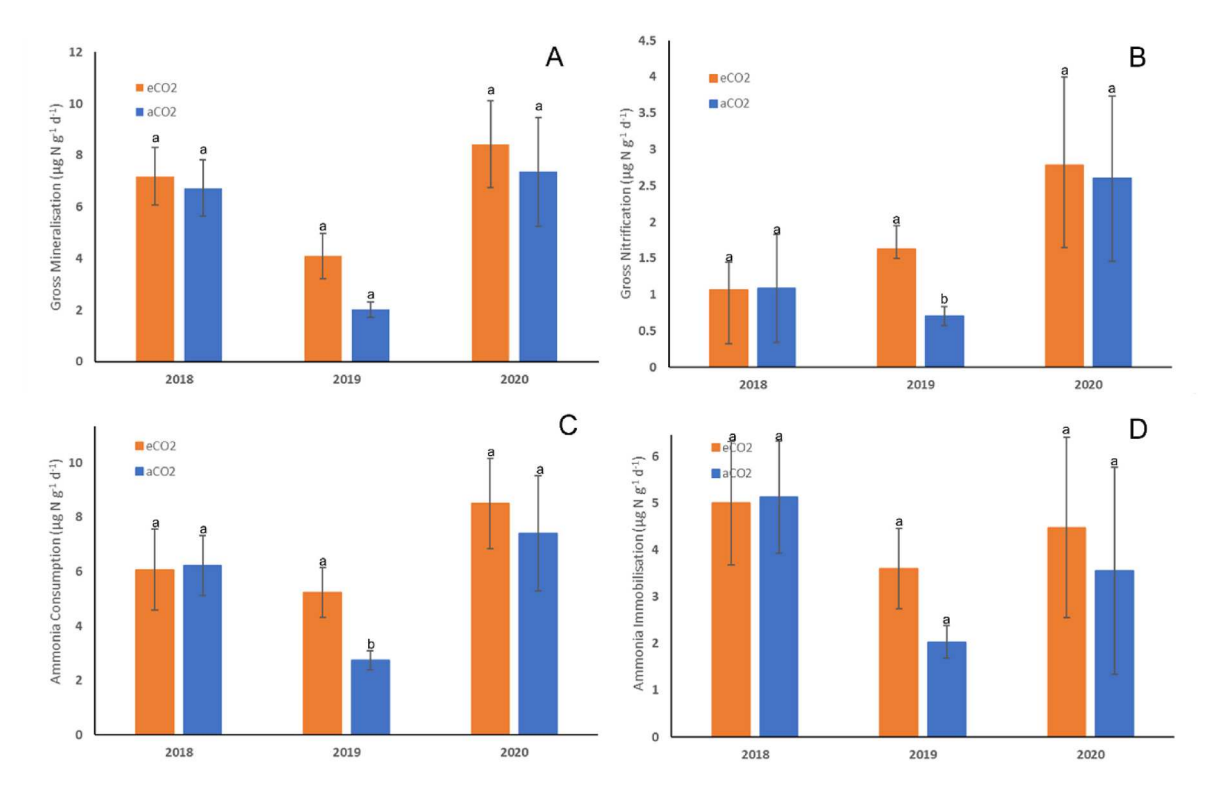


Fig. 2. Gross mineralisation (A), gross nitrification (B), gross ammonia consumption (C) and ammonia immobilisation (D) rates in eCO₂ (fumigated) and aCO₂ (control) soils from the FACE oak woodland in Staffordshire. Data are means \pm SE for each sampled growth seasons between 2018 and 2020. Similar lower case letters indicate no significant difference (p > 0.05) of the means between eCO₂ and aCO₂ treatments according to the Mann-Whitney test.

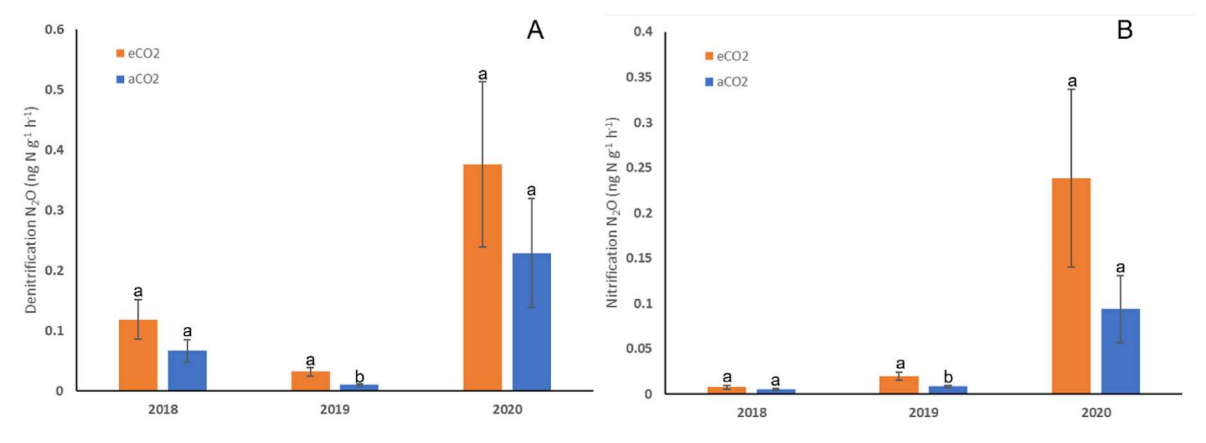


Fig. 3. Nitrous oxide emission due to denitrification (A) and nitrification (B) in eCO₂ (fumigated) and aCO₂ (control) soils from the FACE oak woodland in Staffordshire. Data are means \pm SE for each sampled growth seasons between 2018 and 2020. Similar lower case letters indicate no significant difference (p > 0.05) of the means between eCO₂ and aCO₂ treatments according to the Mann-Whitney test.

denitrification), was not measured under our experimental conditions. Comparing N_2O emission rates between sampled years, only in 2020 N_2O emission was higher than in the two previous years, an apparent trend following the tripling of gross nitrification rates between 2018 and 2020 (Fig. 2B and 3A&B), but it also follows the increase in the soil nitrate pool observed in 2020 (Table S1).

3.4. Potential N_2O emission under two soil moisture regimes

The parallel soil incubation experiment without the addition of 15 N tracers confirmed that eCO₂ soils emitted more N₂O compared to the aCO₂ soils, and this difference was statistically significant (p < 0.05; Fig. 4C). Increasing the typical summer soil moisture from 23% to 50%

did not have a significant effect on N_2O emissions, (p>0.05; Fig. 4E,F, G).Interestingly, the highest N_2O emission was observed on the first day of the incubation and decreased thereafter with the last day of the incubation showing N_2O consumption, a likely effect of lack of external N supply.

3.5. Controlling factors

Principal Component Analysis (PCA) of soil physico-chemical variables across the three sampling seasons (n=90), was employed to separate fumigated and control arrays based on the maximum variance explained by their soil properties. The PCA identified two components with eigenvalues larger than 1 (PC1: 3.514 & PC2: 1.159), which

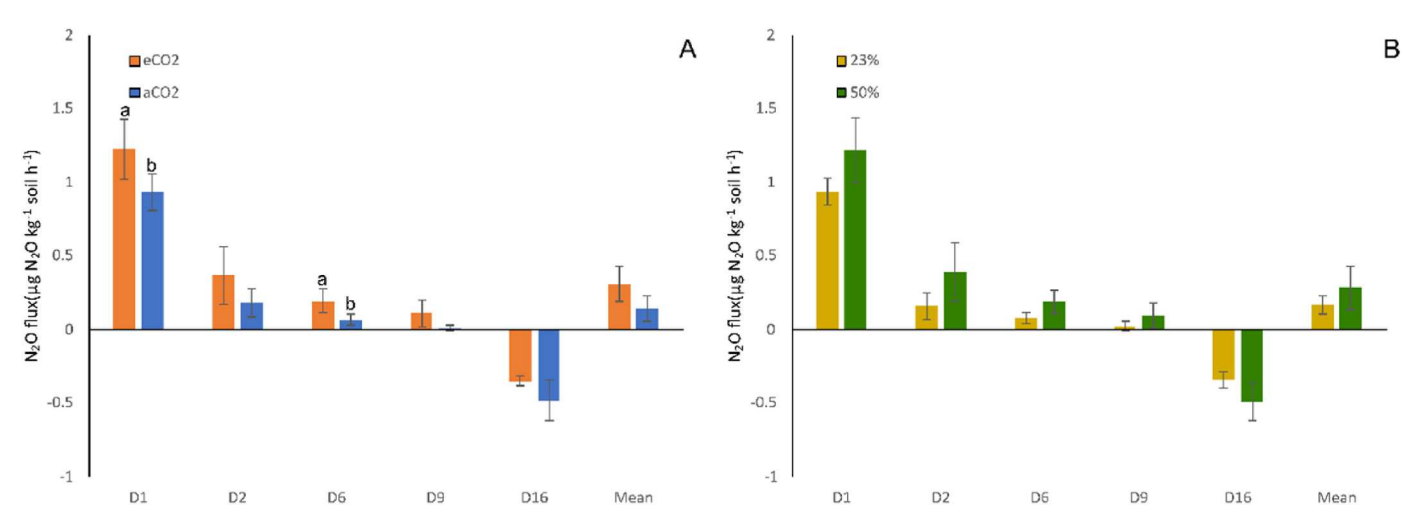


Fig. 4. Elevated CO_2 fumigation (eCO₂) and ambient (aCO₂) treatment interactions for potential N_2O fluxes (A) and lower (23%) and higher volumetric moisture (50%) treatment interactions for N_2O fluxes (B) during laboratory incubations with no N additions over 16 d. Data are presented as mean values \pm standard error (n = 18). Lower case letters indicate a statistically significant difference (p < 0.05) among the different treatment by two-sample T test.

together explained 78% of the total variance within the data set. The soil moisture, nitrate content, total %N and %C correlated significantly (p < 0.01) with the positive axis of the first principal component (PC1) explaining 59% of the observed variance in the overall data. The variable soil δ^{15} N correlated with the positive axis of the second principal component (PC2), while soil δ^{13} C correlated with the negative axis of PC2, which explained an additional 19% of the variance in the dataset (Fig. 5). Cluster centroids (average score on each component, with standard errors) for each array are also presented in Fig. 5. Arrays 1,2,4

and 5 appear to overlap considerably along both PC1 & 2, and only fumigated array 6 and control array 3 seem distinctly different along both axes. However, if the pairing of the arrays is also taken into account, then arrays 1 & 3 as well as arrays 5 & 6 are separated along the bi-plot axes and only arrays 2 & 4 are overlapping. Fumigated arrays (1, 4, and 6) are more closely related with the increasing nitrogen and carbon contents, as well as moisture along PC1, while they also differentiate along PC2 with higher soil δ^{15} N and more depleted soil δ^{13} C. Linear regression analysis between the principal component axes as

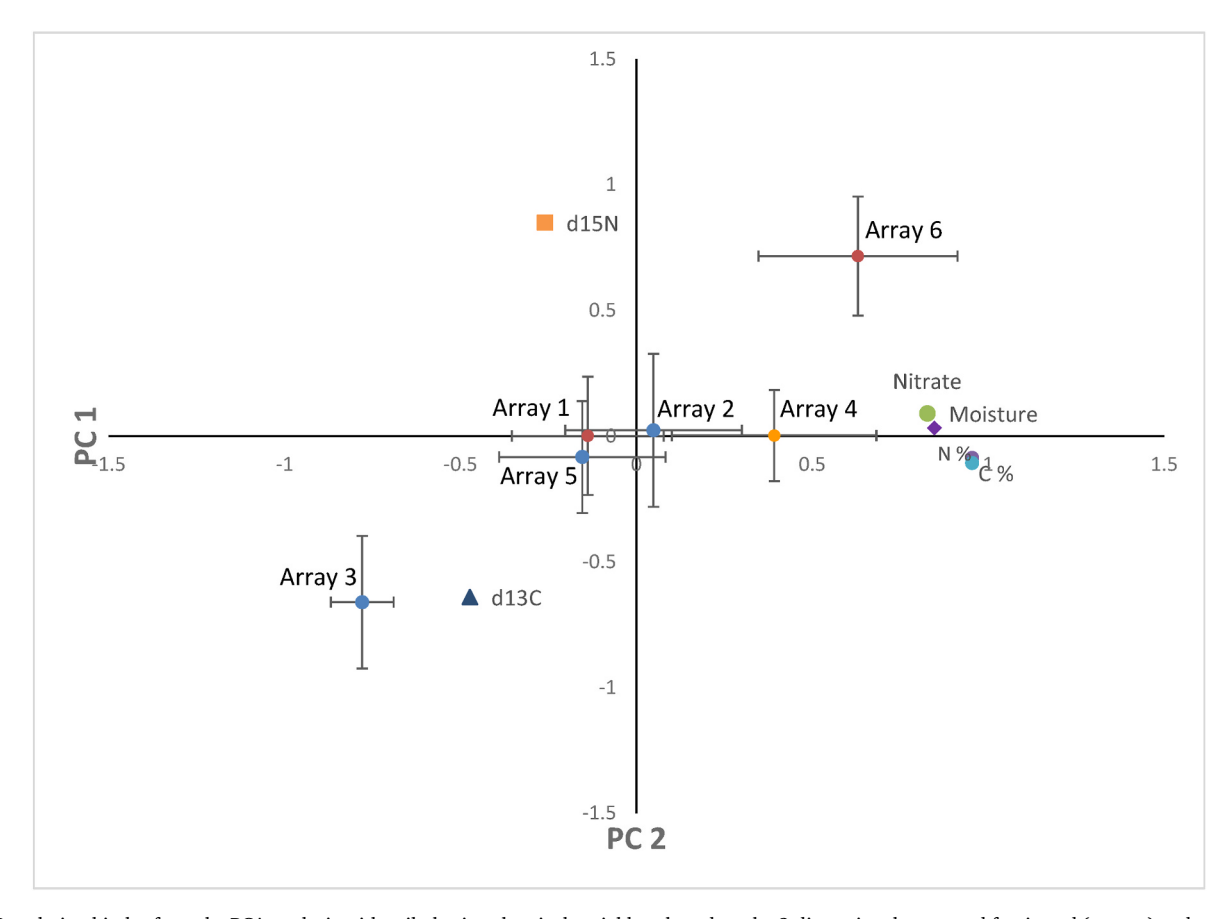


Fig. 5. Correlation bi-plot from the PCA analysis with soil physico-chemical variables plotted on the 2-dimensional space and fumigated (orange) and control (blue) arrays represented by cluster centroids (average score on each component, with standard errors).

independent variables (PCR) and the dependent variables of gross mineralisation and nitrification, as well as nitrous oxide emissions due to denitrification and nitrification showed significant regressions with primarily PC1 (representing soil C & N contents), which explained 21–28% of the variance in the key nitrogen transformation processes (Table 3).

4. Discussion

This study is the first to assess N transformations and N_2O fluxes in a mature oak dominated temperate forest following four initial years of CO_2 fumigation since 2017. There have been numerous, and varying, observations of N cycling in young forests as reviewed by De Graaff et al., (2006) (Rütting and Andresen, 2015), however, only one other FACE experiment has been conducted in a mature forest, albeit P limited; Eucalyptus dominated forests near Sydney, Australia (Euc-FACE (Andresen et al., 2020; Hasegawa et al., 2016; Martins et al., 2021);). Given the potential impact of disturbance on young forests on nutrient cycling under e CO_2 , it is essential to extend observations in undisturbed, mature forests, already at assumed "equilibrium" (Norby et al., 2016; Norby and Zak, 2011). These findings serve to enhance understanding of how N cycling in a mature forest responds in initial years under CO_2 fumigation.

According to our PCR analysis, the key soil properties of C & N content indicated an effect on N transformations following the first three years of eCO2 fumigation. Consistently, the soil ammonium pool was higher under eCO2, which, alongside the trend towards increased soil δ^{15} N, provided initial evidence for an up-regulated N turnover under eCO₂. Further, increases in soil labile DOC support previous findings at BIFoR-FACE (Gardner et al., 2022), and in studies elsewhere (Hasegawa et al., 2016; Phillips et al., 2011), of increased C entering the forest and allocation belowground. An increase in exudation of C by roots at BIFoR-FACE, which has already been observed (unpublished data), will contribute to increases in belowground C availability, priming the microbial community (Dijkstra et al., 2013; Hoosbeek et al., 2004). Soil C and N drove the separation of two of the three paired arrays, indicating these were treatment effects and not due to pre-existing differences in arrays. Enhancements in photosynthesis at BIFoR-FACE and no change in foliar N under eCO2 indicated soil nutrient availability was not yet limiting above ground processes, as has been observed in previous FACE experiments (Crous et al., 2008; Gardner et al., 2022). The moderate N deposition at BIFoR FACE (\sim 25 kg N ha⁻¹ y⁻¹ (Tomlinson et al., 2020); may also buffer any increases in a fast track N limitation. Gravimetric soil moisture measured at the time of soil sampling was also a key variable separating ambient and elevated treatments, with higher moisture content under eCO2. Previous studies have observed increased soil moisture, linked to increased water use efficiency (WUE), arising from reduced evapotranspiration as a consequence of decreasing stomatal conductance (Ainsworth and Rogers, 2007). Further work at BIFOR-FACE to determine any effects of eCO₂ on WUE is required to test this potential influence on soil moisture, and subsequently nutrient cycling, given the limited investigation of soil moisture dynamics herein (MacKenzie et al., 2021).

Even though all determined N cycling processes were on average and consistently across the 3 sampled years higher under eCO $_2$; however,

Table 3 Principal component regression between soil nitrogen cycling processes and PC1 & 2 axes of the PCA analysis. r^2 linear regression coefficient of determination, p; probability level, n=90.

Nitrogen Transformations	$PC1 - r^2$	p-value	PC2 - r ²	p-value
Gross Mineralisation	0.241	< 0.001	0.071	0.011
Gross Nitrification	0.210	< 0.001	0.002	0.662
Denitrification N ₂ O	0.250	< 0.001	0.006	0.464
Nitrification N ₂ O	0.284	< 0.001	0.014	0.279

due to high spatial and temporal variability between arrays and sampled years, these differences were not statistically significant at 95% confidence interval, except in 2019 when gross nitrification and ammonia consumption were significantly high under eCO2. (Table 2). A potential enhancement in N cycling may be supported by the decreased MRT for both ammonium and nitrate under eCO2. This finding is similar to previous work at Aspen-FACE, where mineralisation doubled and immobilisation increased four-fold under eCO₂, with year-to-year variation in the size of the response (Holmes et al., 2006). However, in P-limited (Euc-FACE), and P and N-limited (Web-FACE) mature forests, no enhancement of mineralisation or immobilisation has been observed (Andresen et al., 2020; Schleppi et al., 2019) due to eCO2. The lack of response at these settings was likely due to co-limitation. In contrast at BIFOR-FACE, where the C:N ratio of \sim 16–17 in the upper soil layers indicate moderate limitation, there was a potential enhanced response of N mineralisation and immobilisation under eCO2. This is consistent with eCO2 experiments in other ecosystems (e.g. grassland, desert), where meta-analysis has confirmed a general trend towards enhanced response of gross immobilisation and mineralisation under eCO₂, particularly in N limited ecosystems (Rütting and Andresen, 2015). At BIFOR-FACE, it is suggested there are two potential mechanisms via which the eCO2 may upregulate the N cycle. Firstly, the direct effect of increased C availability, from increases in photosynthesis (Gardner et al., 2021). Regression analyses (Fig. S1) indicated mineralisation rates increased with higher C content for both aCO2 and eCO2 treatments to the same degree, although rates were not significantly different (95% CI). Hence despite differences in DOC and %C content between the two treatments, we cannot attribute with high confidence any upregulation of N cycling processes to this direct eCO₂ fertilisation effect. The alternative suggestion is the indirect effect of increased N demand, under eCO₂ treatment, reflecting higher N content of green leaf biomass (Gardner et al., 2022), resulted in upregulation of N cycling processes. This is supported by the stronger positive linear relationship of N mineralisation rate with %N content (Fig. S2) under eCO₂ (23 μg g⁻¹ $day^{-1}\%^{-1}$) vs. aCO₂ (-1.2 µg g⁻¹ $day^{-1}\%^{-1}$). Modest increases in N cycling processes, combined with higher C/N ratio under eCO2, suggested high competition for N released following the indirect effect of eCO2 and a potential tightening of the N cycle. All changes in N cycling transformations were small, with inter-year variability observed (Appendix A). It has been suggested that the variability in soil N processes is larger than the change due to treatment effects, where atmospheric CO₂ fumigation has increased by only \sim 37%, thus limiting the observation of significant responses (Zak et al., 2000, 2007). However, the magnitude of response for soil N transformations were comparable to the increase in atmospheric CO2 and enhanced CO2 uptake of 23% by the dominant oak trees at BIFoR-FACE (Gardner et al., 2021) Further, the magnitude of the response of N cycling processes under eCO2 is also influenced by site factors, such as climate (Holmes et al., 2006; Zak et al., 2000).

Under both aCO2 and eCO2 treatments, gross mineralisation was ca. 4 times higher than nitrification, consistent with the higher observed soil NH₄ and higher MRT for ammonium relative to nitrate. While immobilisation dominated ammonium consumption (68% for both treatments across years), there was a year-on-year decrease in the proportion accounted for by immobilisation, alongside an increase in gross nitrification rates. Nitrification exhibited a positive relative response for eCO₂ (0.20), however, there was a comparable response of mineralisation (0.19), indicting the change in the relative ratio of nitrification and immobilisation contributing to NH₄ consumption was not associated with CO₂ fumigation. Similarly, the relative response of mineralisation (0.20) and ammonium consumption (0.19) was also comparable, indicating no increase in consumption relative to production under eCO2 compared to ambient, which may have reduced plant N availability (Hungate et al., 2003; Rütting and Andresen, 2015). This finding was consistent with previous observations of no effect of eCO₂ on foliar N content at BIFoR-FACE in the first three years since the start of fumigation (Gardner et al., 2021, 2022).

Fumigation with elevated CO₂ had an overall positive effect on potential N2O emissions, and this was observed particularly under nitrate treatments and to a lesser extent under ammonium treatments. However, at the no tracer addition experiment, there was a significant stimulation of N2O emission under eCO2. This finding is in contrast to our initial hypothesis of downregulation of N2O emissions due to the Nlimiting soil conditions at the mature oak forest as well as the increased N demand by trees. Previous studies that investigated N₂O emissions under FACE conditions in forest ecosystems reported no significant differences between eCO₂ and control treatments (Phillips et al., 2001) or a negative trend (Martins et al., 2021), which were attributed mainly to N-limitation during the tree growth season (Phillips et al., 2001), or soil moisture and P co-limitation restricting N mineralisation under the dryland conditions at the EucFACE experiment (Martins et al., 2021). However, our observations of a modest increase in N-mineralisation as well as significant increases in belowground C allocation, indicated by soil DOC, and increased soil moisture (Ainsworth and Rogers, 2007), point towards the stimulation of microbial N processing and thus N2O emission (Qiu et al., 2019). This is further supported by the significant regression between N2O and PC1 (Fig. 5), largely defined by the soil moisture, N and carbon content variables.

Increased N2O emissions under CO2 fumigation have been consistently reported in grassland FACE experiments (Baggs et al., 2003; Kammann et al., 2008; Moser et al., 2018) and largely explained by the stimulating effect of the additional belowground allocated C on soil organic matter mineralisation, although often under non N-limiting conditions. Interestingly, we have also observed almost doubling of N2O emissions under eCO₂, which agrees with the observations after 25 years of CO₂ fumigation at the Giessen Free Air CO₂ Enrichment (GiFACE) permanent grassland (Moser et al., 2018), although the magnitudes of N2O fluxes are very different. Low net N2O emissions from largely aerobic natural forest soils are typical in mature temperate (Sgouridis and Ullah, 2017) and tropical forests (Martins et al., 2021), where low substrate availability and lack of sub-oxic conditions limits denitrification-derived N2O emissions (Butterbach-Bahl et al., 2013). In our case, N2O fluxes were 3-4 orders of magnitude lower than gross mineralisation rates, while the acidic pH (\sim <4) is likely limiting autotrophic nitrification further (Butterbach-Bahl et al., 2013; Nicol et al., 2008). Both soil conditions combined reduce nitrification derived N2O emissions, as well as the supply of nitrate to denitrification. Our labelling experiment confirmed denitrification as the main source of N2O, emitting twice as much nitrous oxide than nitrification in eCO₂ soils, and 3 times as much in control soils. There was no indication (no ammonium enrichment under the ${}^{15}\mathrm{NO}_3^-$ treatment – data not shown) that dissimilatory nitrate reduction to ammonium (DNRA) may play a quantitatively important role as an N2O source in these aerobic forest soils. DNRA in terrestrial ecosystems has been shown to be important under a high C/N ratio but also higher soil moisture (Sgouridis et al., 2011) than in the BiFOR-FACE forest soils. While natural abundance isotopomer stable isotope approaches (Pérez et al., 2006) are non-invasive and can provide valuable information on which processes may be involved in N₂O production, they are inconclusive on their own and cannot provide quantification information (Baggs, 2008). Stable isotope enrichment approaches that involve the addition of labelled ammonium and nitrate to soil have been the most reliable quantification method of N₂O source partitioning so far providing information for various potential N2O sources (Baggs et al., 2003). During our incubations, we did not discriminate between autotrophic and heterotrophic nitrification (nitrate produced from the oxidation of organic N), with the latter recently shown as quantitatively important in acidic forest soils in both temperate and subtropical biomes (Stange et al., 2013; Zhang et al., 2015, 2018). Heterotrophic nitrification mainly occurs as part of fungi metabolism and there are reports that it may persist under low pH better than ammonia oxidising bacteria (De Boer and Kowalchuk, 2001). Considering that heterotrophic nitrification is favoured by increasing soil organic carbon and an increased C/N ratio, alongside the fact that

ectomycorrhizal fungi are becoming more abundant in fumigated soils in BiFOR-FACE (personal communication), it is warranted further investigation whether heterotrophic nitrification may become more prevalent as an N_2O source as a result of CO_2 fumigation.

5. Implications and future considerations

For the first time we show that in a mature temperate oak dominated forest, soil N cycling was potentially enhanced during the first four years of eCO2 fumigation. The relative increase in gross N mineralisation under eCO₂, and correlation with soil %N, alongside previous evidence of sustained plant N supply in addition to enhanced microbial N immobilisation supported upregulation of N cycling. These findings reflect upregulation in the initial years of fumigation, however, previous FACE experiments in young forests have exhibited progressive nitrogen limitation (Luo et al., 2004; Norby and Zak, 2011). Whilst northern temperate forests in the western hemisphere have been exposed to enhanced atmospheric reactive nitrogen (Nr) deposition in the 20th century, the contemporary gradual decline in Nr deposition in the UK since 2000 coupled with increasing atmospheric CO₂ is likely to result in progressive nitrogen limitation (Tipping et al., 2017). These results are important for elucidating how long N supply will be sustained before N limitation is manifested with implications for carbon uptake by temperate forests under future climates. Future, longer term investigation of N cycling processes at BIFoR-FACE will reveal if any potential upregulation of N cycling will support plant N supply. This is critical to help reduce the substantial uncertainty reported recently (2022) by IPCC regarding N availability and the land carbon sink response under future climates, where experimental data on northern mature temperate forests are grossly lacking (IPCC, 2022; AR6 WG1).

Furthermore, increased N_2O emission under eCO₂, with and without nutrient substrates addition, pointed towards the potential for positive feedbacks on N_2O emissions. Denitrification was confirmed as the main N_2O source as autotrophic nitrification could be inhibited by the acidic soil conditions. Whilst forests are important sinks for carbon (Crowther et al., 2015; Pan et al., 2011), global forests contribute \sim 60% of the total natural source emissions of N_2O (Tian et al., 2020), thus even minor shifts in N_2O fluxes under eCO₂ can have substantial positive feedback for the net global warming potential of forests. Future work should provide an *in situ* N_2O flux budget, to estimate potential positive feedbacks on C sequestration in mature temperate forests.

Declaration of competing interest

The authors declare that they have no known competing financial interests or personal relationships that could have appeared to influence the work reported in this paper.

Data availability

Data will be made available on request.

Acknowledgements

The authors would like to extend thanks to the Technical Team at BIFOR-FACE(Dr. K Hart, P. Miles, N. Harper, T. Downes, Dr. G. Curioni and G. Denny), who maintains and operates the experimental FACE infrastructure and provided support in field work for research work under this project. The authors would like to acknowledge the presubmission reviews by Prof. I. P. Hartley at Exeter University, which helped in improving the manuscript. BIFOR-FACE facility is supported by the JABBS Trust and the University of Birmingham, which made this research possible. We acknowledge generous financial support provided by British Council, Newton Fund (grant #261867079), the Thailand Research Fund (grant # PDG60W0017, enabling S. Cotchim to travel to BIFOR-FACE from The Prince of Songkla University for starting this

research in 2018) and the UKRI-Natural Environment Research Council grants (NE/T000449/1; and NE/T012323/1) for continuation of this research through 2019–2020.

Appendix A. Supplementary data

Supplementary data to this article can be found online at https://doi.org/10.1016/j.soilbio.2023.109072.

References

- Ainsworth, E.A., Long, S.P., 2005. What have we learned from 15 years of free-air CO2 enrichment (FACE)? A meta-analytic review of the responses of photosynthesis, canopy properties and plant production to rising CO2. New Phytologist 165, 351–372.
- Ainsworth, E.A., Rogers, A., 2007. The response of photosynthesis and stomatal conductance to rising [CO2]: mechanisms and environmental interactions. Plant, Cell and Environment 30, 258–270.
- Ambus, P., Robertson, G.P., 1999. Fluxes of CH4 and N2O in aspen stands grown under ambient and twice-ambient CO2. Plant and Soil 209, 1–8.
- Ambus, P., Zechmeister-Boltenstern, S., Butterbach-Bahl, K., 2006. Sources of nitrous oxide emitted from European forest soils. Biogeosciences 3, 135–145.
- Andresen, L.C., Carrillo, Y., Macdonald, C.A., Castañeda-Gómez, L., Bodé, S., Rütting, T., 2020. Nitrogen dynamics after two years of elevated CO2 in phosphorus limited Eucalyptus woodland. Biogeochemistry 150, 297–312.
- Arah, J.R.M., 1997. Apportioning nitrous oxide fluxes between nitrification and denitrification using gas-phase mass spectrometry. Soil Biology and Biochemistry 29, 1295–1299.
- Baggs, E.M., Richter, M., Cadisch, G., Hartwig, U.A., 2003. Denitrification in grass swards is increased under elevated atmospheric CO2. Soil Biology and Biochemistry 35, 729–732.
- Baggs, E.M., 2008. A review of stable isotope techniques for N₂O source partitioning in soils: recent progress, remaining challenges and future considerations. Rapid Communications in Mass Spectrometry 22 (11), 1664–1672. https://doi.org/ 10.1002/rcm_3456.
- Brooks, P.D., Stark, J.M., McInteer, B.B., Preston, T., 1989. Diffusion method to prepare soil extracts for automated Nitrogen-15 analysis. Soil Science Society of America Journal 53, 1707–1711.
- Butterbach-Bahl, K., Baggs, E.M., Dannenmann, M., Kiese, R., Zechmeister-Boltenstern, S., 2013. Nitrous oxide emissions from soils: how well do we understand the processes and their controls? Philosophical Transactions of the Royal Society B: Biological Sciences 368.
- Carnol, M., Hogenboom, L., Jach, M.E., Remacle, J., Ceulemans, R., 2002. Elevated atmospheric CO2 in open top chambers increases net nitrification and potential denitrification. Global Change Biology 8, 590–598.
- Crous, K.Y., Walters, M.B., Ellsworth, D.S., 2008. Elevated CO2 concentration affects leaf photosynthesis–nitrogen relationships in Pinus taeda over nine years in FACE. Tree Physiology 28, 607–614.
- Crowther, T.W., Glick, H.B., Covey, K.R., Bettigole, C., Maynard, D.S., Thomas, S.M., et al., 2015. Mapping tree density at a global scale. Nature 525, 201–205. Davidson, E.A., Hart, S.C., Firestone, M.K., 1992. Internal cycling of nitrate in soils of a
- Davidson, E.A., Hart, S.C., Firestone, M.K., 1992. Internal cycling of nitrate in soils of a mature coniferous forest. Ecology 73, 1156.
- De Boer, W., Kowalchuk, G.A., 2001. Nitrification in acid soils: micro-organisms and mechanisms. Soil Biology and Biochemistry 33, 853–866.
- De Graaff, M.-A., Van Groenigen, K.-J., Six, J., Hungate, B., Van Kessel, C., 2006. Interactions between plant growth and soil nutrient cycling under elevated CO2: a meta-analysis. Global Change Biology 12, 2077–2091.
- Delucia, E.H., Callaway, R.M., Thomas, E.M., Schlesinger, W.H., 1997. Mechanisms of phosphorus acquisition for ponderosa pine seedlings under high CO2and temperature. Annals of Botany 79, 111–120.
- Dieleman, W.I.J., Luyssaert, S., Rey, A., De Angelis, P., Barton, C.V.M., Broadmeadow, M. S.J., et al., 2010. Soil [N] modulates soil C cycling in CO2-fumigated tree stands: a meta-analysis. Plant, Cell and Environment 33, 2001–2011.
- Dijkstra, F., Carrillo, Y., Pendall, E., Morgan, J., 2013. Rhizosphere priming: a nutrient perspective. Frontiers in Microbiology 4.
- Fransson, P.M.A., Johansson, E.M., 2010. Elevated CO2 and nitrogen influence exudation of soluble organic compounds by ectomycorrhizal root systems. FEMS Microbiology Ecology 71, 186–196.
- Friedlingstein, P., O'Sullivan, M., Jones, M.W., Andrew, R.M., Hauck, J., Olsen, A., et al., 2020. Global carbon budget 2020. Earth System Science Data 12, 3269–3340.
- Gardner, A., Ellsworth, D.S., Crous, K.Y., Pritchard, J., MacKenzie, A.R., 2021. Is photosynthetic enhancement sustained through three years of elevated CO2 exposure in 175-year-old Quercus robur? Tree Physiology 42, 130–144.
- Gardner, A., Ellsworth, D.S., Pritchard, J., MacKenzie, A.R., 2022. Are Chlorophyll Concentrations and Nitrogen across the Vertical Canopy Profile Affected by Elevated CO2 in Mature Quercus Trees? Trees.
- Hagedorn, F., Bucher, J.B., Tarjan, D., Rusert, P., Bucher-Wallin, I., 2000. Responses of N fluxes and pools to elevated atmospheric CO2 in model forest ecosystems with acidic and calcareous soils. Plant and Soil 224, 273–286.
- Hart, K.M., Curioni, G., Blaen, P., Harper, N.J., Miles, P., Lewin, K.F., et al., 2020. Characteristics of free air carbon dioxide enrichment of a northern temperate mature forest. Global Change Biology 26, 1023–1037.

- Hart, S.C., Nason, G.E., Myrold, D.D., Perry, D.A., 1994. Dynamics of gross nitrogen transformations in an old-growth forest: the carbon connection. Ecology 75, 880–891.
- Hasegawa, S., Macdonald, C.A., Power, S.A., 2016. Elevated carbon dioxide increases soil nitrogen and phosphorus availability in a phosphorus-limited Eucalyptus woodland. Global Change Biology 22, 1628–1643.
- Hendrey, G.R., Ellsworth, D.S., Lewin, K.F., Nagy, J., 1999. A free-air enrichment system for exposing tall forest vegetation to elevated atmospheric CO2. Global Change Biology 5, 293–309.
- Holmes, W.E., Zak, D.R., Pregitzer, K.S., King, J.S., 2006. Elevated CO2 and O3 alter soil nitrogen transformations beneath trembling aspen, paper birch, and sugar maple. Ecosystems 9, 1354–1363.
- Hoosbeek, M.R., Lukac, M., van Dam, D., Godbold, D.L., Velthorst, E.J., Biondi, F.A., et al., 2004. More new carbon in the mineral soil of a poplar plantation under Free Air Carbon Enrichment (POPFACE): cause of increased priming effect? Global Biogeochemical Cycles 18.
- Hungate, B.A., Dukes, J.S., Shaw, M.R., Luo, Y., Field, C.B., 2003. Nitrogen and climate change. Science 302, 1512–1513.
- Jackson, R.B., Cook, C.W., Pippen, J.S., Palmer, S.M., 2009. Increased belowground biomass and soil CO2 fluxes after a decade of carbon dioxide enrichment in a warmtemperate forest. Ecology 90, 3352–3366.
- Jiang, M., Medlyn, B.E., Drake, J.E., Duursma, R.A., Anderson, I.C., Barton, C.V.M., et al., 2020. The fate of carbon in a mature forest under carbon dioxide enrichment. Nature 580, 227–231.
- Jilling, A., Keiluweit, M., Gutknecht, J.L.M., Grandy, A.S., 2021. Priming mechanisms providing plants and microbes access to mineral-associated organic matter. Soil Biology and Biochemistry 158, 108265.
- Johansson, E.M., Fransson, P.M.A., Finlay, R.D., van Hees, P.A.W., 2009. Quantitative analysis of soluble exudates produced by ectomycorrhizal roots as a response to ambient and elevated CO2. Soil Biology and Biochemistry 41, 1111–1116.
- Kammann, C., Müller, C., Grünhage, L., Jäger, H.-J., 2008. Elevated CO2 stimulates N2O emissions in permanent grassland. Soil Biology and Biochemistry 40, 2194–2205.
- Keenan, R.J., Reams, G.A., Achard, F., de Freitas, J.V., Grainger, A., Lindquist, E., 2015. Dynamics of global forest area: results from the FAO global forest resources assessment 2015. Forest Ecology and Management 352, 9–20.
- Kirkham, D., Bartholomew, W.V., 1954. Equations for following nutrient transformations in soil, utilising tracer data. Soil Science Society of America Proceedings 18, 33–34. Knowles, R., 1982. Denitrification. Microbiological Reviews 46, 43–70.
- Kuzyakov, Y., 2002. Review: factors affecting rhizosphere priming effects. Journal of Plant Nutrition and Soil Science 165, 382–396.
- Luo, Y., Su, B., Currie, W.S., Dukes, J.S., Finzi, A., Hartwig, U., et al., 2004. Progressive nitrogen limitation of ecosystem responses to rising atmospheric carbon dioxide. BioScience 54, 731–739.
- MacKenzie, A.R., Krause, S., Hart, K.M., Thomas, R.M., Blaen, P.J., Hamilton, R.L., et al., 2021. BIFOR FACE: water–soil–vegetation–atmosphere data from a temperate deciduous forest catchment, including under elevated CO2. Hydrological Processes 35. e14096.
- Martins, C.S.C., Nazaries, L., Delgado-Baquerizo, M., Macdonald, C.A., Anderson, I.C., Singh, B.K., 2021. Rainfall frequency and soil water availability regulate soil methane and nitrous oxide fluxes from a native forest exposed to elevated carbon dioxide. Functional Ecology 35, 1833–1847.
- Matson, A., Pennock, D., Bedard-Haughn, A., 2009. Methane and nitrous oxide emissions from mature forest stands in the boreal forest, Saskatchewan, Canada. Forest Ecology and Management 258, 1073–1083.
- Moser, G., Gorenflo, A., Brenzinger, K., Keidel, L., Braker, G., Marhan, S., et al., 2018. Explaining the doubling of N2O emissions under elevated CO2 in the Giessen FACE via in-field 15N tracing. Global Change Biology 24, 3897–3910.
- Mulvaney, R.L., 1984. Determination of 15N-labeled dinitrogen and nitrous oxide with triple-collector mass spectrometers. Soil Science Society of America Journal 48, 690–692.
- Nicol, G.W., Leininger, S., Schleper, C., Prosser, J.I., 2008. The influence of soil pH on the diversity, abundance and transcriptional activity of ammonia oxidizing archaea and bacteria. Environmental Microbiology 10, 2966–2978.
- Norby, R.J., De Kauwe, M.G., Domingues, T.F., Duursma, R.A., Ellsworth, D.S., Goll, D.S., et al., 2016. Model–data synthesis for the next generation of forest free-air CO2 enrichment (FACE) experiments. New Phytologist 209, 17–28.
- Norby, R.J., Zak, D.R., 2011. Ecological lessons from free-air CO2 enrichment (FACE) experiments. Annual Review of Ecology, Evolution and Systematics 42, 181–203.
- Nowak, R.S., Ellsworth, D.S., Smith, S.D., 2004. Functional responses of plants to elevated atmospheric CO2– do photosynthetic and productivity data from FACE experiments support early predictions? New Phytologist 162, 253–280.
- Ochoa-Hueso, R., Hughes, J., Delgado-Baquerizo, M., Drake, J.E., Tjoelker, M.G., Piñeiro, J., et al., 2017. Rhizosphere-driven increase in nitrogen and phosphorus availability under elevated atmospheric CO2 in a mature Eucalyptus woodland. Plant and Soil 416, 283–295.
- Pan, Y., Birdsey, R.A., Fang, J., Houghton, R., Kauppi, P.E., Kurz, W.A., et al., 2011. A large and persistent carbon sink in the world's forests. Science 333, 988–993.
- Pérez, T., Garcia-Montiel, D., Trumbore, S., Tyler, S., Camargo, P.D., Moreira, M., Cerri, C., 2006. Nitrous oxide nitrification and denitrification 15N enrichment factors from Amazon forest soils. Ecological Applications 16 (6), 2153–2167. https://doi.org/10.1890/1051-0761(2006)016[2153:NONADN]2.0.CO;2.
- Phillips, R.L., Whalen, S.C., Schlesinger, W.H., 2001. Influence of atmospheric CO2 enrichment on nitrous oxide flux in a temperate forest ecosystem. Global Biogeochemical Cycles 15, 741–752.

- Phillips, R.P., Bernhardt, E.S., Schlesinger, W.H., 2009. Elevated CO2 increases root exudation from loblolly pine (Pinus taeda) seedlings as an N-mediated response. Tree Physiology 29, 1513–1523.
- Phillips, R.P., Finzi, A.C., Bernhardt, E.S., 2011. Enhanced root exudation induces microbial feedbacks to N cycling in a pine forest under long-term CO2 fumigation. Ecology Letters 14, 187–194.
- Phillips, R.P., Meier, I.C., Bernhardt, E.S., Grandy, A.S., Wickings, K., Finzi, A.C., 2012. Roots and fungi accelerate carbon and nitrogen cycling in forests exposed to elevated CO2. Ecology Letters 15, 1042–1049.
- Piñeiro, J., Ochoa-Hueso, R., Delgado-Baquerizo, M., Dobrick, S., Reich, P.B., Pendall, E., et al., 2017. Effects of elevated CO2 on fine root biomass are reduced by aridity but enhanced by soil nitrogen: a global assessment. Scientific Reports 7, 15355.
- Qiu, Y., Jiang, Y., Guo, L., Zhang, L., Burkey, K.O., Zobel, R.W., et al., 2019. Shifts in the composition and activities of denitrifiers dominate CO2 stimulation of N2O emissions. Environmental Science and Technology 53, 11204–11213.
- Rütting, T., Andresen, L.C., 2015. Nitrogen cycle responses to elevated CO2 depend on ecosystem nutrient status. Nutrient Cycling in Agroecosystems 101, 285–294.
- Schleppi, P., Körner, C., Klein, T., 2019. Increased nitrogen availability in the soil under mature picea abies trees exposed to elevated CO2 concentrations. Frontiers in Forests and Global Change 2.
- Sgouridis, F., Heppell, C.M., Wharton, G., Lansdown, K., Trimmer, M., 2011.

 Denitrification and dissimilatory nitrate reduction to ammonium (DNRA) in a temperate re-connected floodplain. Water Research 45, 4909–4922.
- Sgouridis, F., Stott, A., Ullah, S., 2016. Application of the 15N gas-flux method for measuring in situ N2 and N2O fluxes due to denitrification in natural and seminatural terrestrial ecosystems and comparison with the acetylene inhibition technique. Biogeosciences 13, 1821–1835.
- Sgouridis, F., Ullah, S., 2015. Relative magnitude and controls of in situ N2 and N2O fluxes due to denitrification in natural and seminatural terrestrial ecosystems using 15N tracers. Environmental Science and Technology 49, 14110–14119.
- Sgouridis, F., Ullah, S., 2017. Soil greenhouse gas fluxes, environmental controls, and the partitioning of N2O sources in UK natural and seminatural land use types. Journal of Geophysical Research: Biogeosciences 122, 2617–2633.

- Stange, C.F., Spott, O., Arriaga, H., Menéndez, S., Estavillo, J.M., Merino, P., 2013. Use of the inverse abundance approach to identify the sources of NO and N2O release from Spanish forest soils under oxic and hypoxic conditions. Soil Biology and Biochemistry 57, 451–458.
- Terrer, C., Jackson, R.B., Prentice, I.C., Keenan, T.F., Kaiser, C., Vicca, S., et al., 2019. Nitrogen and phosphorus constrain the CO2 fertilization of global plant biomass. Nature Climate Change 9, 684–689.
- Tian, H., Xu, R., Canadell, J.G., Thompson, R.L., Winiwarter, W., Suntharalingam, P., et al., 2020. A comprehensive quantification of global nitrous oxide sources and sinks. Nature 586, 248–256.
- Tipping, E., Davies, J.A.C., Henrys, P.A., Kirk, G.J.D., Lilly, A., Dragosits, U., et al., 2017. Long-term increases in soil carbon due to ecosystem fertilization by atmospheric nitrogen deposition demonstrated by regional-scale modelling and observations. Scientific Reports 7.
- Tomlinson, S.J., Carnell, E.J., Dore, A.J., Dragosits, U., 2020. Nitrogen Deposition in the UK at 1km Resolution, 1990-2017. NERC Environmental Information Data Centre
- van Groenigen, K.J., Osenberg, C.W., Hungate, B.A., 2011. Increased soil emissions of potent greenhouse gases under increased atmospheric CO2. Nature 475, 214–216.
- Zak, D.R., Holmes, W.E., Finzi, A.C., Norby, R.J., Schlesinger, W.H., 2003. Soil nitrogen cycling under elevated CO2: a synthesis of forest FACE experiments. Ecological Applications 13, 1508–1514.
- Zak, D.R., Holmes, W.E., Pregitzer, K.S., 2007. Atmospheric CO2 and O3 alter the flow of 15N in developing forest ECOsystems. Ecology 88, 2630–2639.
- Zak, D.R., Pregitzer, K.S., King, J.S., Holmes, W.E., 2000. Elevated atmospheric CO2, fine roots and the response of soil microorganisms: a review and hypothesis. New Phytologist 147, 201–222.
- Zhang, J., Müller, C., Cai, Z., 2015. Heterotrophic nitrification of organic N and its contribution to nitrous oxide emissions in soils. Soil Biology and Biochemistry 84, 199–209.
- Zhang, Y., Zhao, W., Cai, Z., Müller, C., Zhang, J., 2018. Heterotrophic nitrification is responsible for large rates of N2O emission from subtropical acid forest soil in China. European Journal of Soil Science 69, 646–654.